JOC Featured Article

Rearrangemements in Piperidine-Derived Nitrogen-Centered Radicals. A Quantum-Chemical Study

Valerije Vrček*,† and Hendrik Zipse‡

Faculty of Pharmacy and Biochemistry, University of Zagreb, A. Kovacica 1, HR-10000 Zagreb, Croatia, and Department of Chemistry and Biochemistry, LMU München, Butenandstr. 13, D-81377 München, Germany

valerije@pharma.hr

Received February 17, 2009

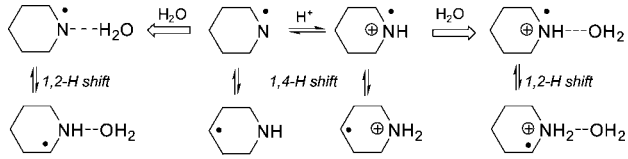

Hydrogen migration reactions in piperidine radicals and their protonated counterparts were studied by quantum chemical calculations. G3B3 and G3(MP2)-RAD levels of theory were used as reference procedures in order to evaluate the efficiency of other computational models. In the gas phase, the 1,4-[N↔C]-H and 1,4-[C↔C]-H shifts are the most feasible rearrangements in the piperidine radical cation and neutral piperidine radical, respectively. However, if one explicit water molecule is well placed to facilitate hydrogen migrations, the 1,2-[N↔C]-H shift becomes the most favorable process in both cases. Three different water-catalyzed [N↔C]-H shift mechanisms were considered for piperidine radical cation, and only one is found to be operative in the case of neutral piperidine radical. We found that explicit solvation and protonation of piperidine-derived radicals strongly influence the overall mechanism of hydrogen migration reactions.

Introduction

N-Chlorination plays an important role in environmental chemistry and biochemistry. A wide variety of biological molecules including amino acids, peptides and proteins,[1] DNA and RNA,[2] as well as glycosamines[3] react with hypochlorous acid (HOCl) or molecular chlorine (Cl_2). The reactions of HOCl/Cl_2 with these nitrogen-containing compounds have been shown to produce chloramines. These latter compounds are relatively unstable intermediates that can undergo several rearrangement processes that depend on both medium and substituent effects.[4−7] Of special importance are reactions in which nitrogen-centered radicals are formed (Scheme 1). These reactive species have been postulated to play a role in the damage of biologically important molecules.[8]

Nitrogen-centered radicals can undergo different intramolecular rearrangements as outlined in Scheme 1. These reactions include intramolecular 1,*n*-hydrogen atom shifts (where $n = 2-8$), in which the corresponding carbon-centered radicals are formed (reaction [**1**]), β-scissions, which result in the cleavage of suitable C−C bonds (reaction [**2**]), and nitrogen atom migration (reaction [**3**]). All these intramolecular rearrangement reactions in nitrogen-centered radicals play an important role in site-selective fragmentations of biologically important molecules such as DNA, glycosaminoglycans, nucleotides, amino acids, or proteins. Chloramines are also generated on reaction of chlorine with numerous inorganic and organic micropollutants during water treatment procedures,[9] and some of these have been shown to have carcinogenic and/or mutagenic properties.[10] Of special importance are pharmaceuticals and personal care products (PPCP), which have been frequently detected in

* To whom correspondence should be addressed. Tel: +385-1-6394441. Fax: +385-1-4856201.
† University of Zagreb.
‡ LMU München.

(1) Hawkins, C. L.; Pattison, D. I.; Davies, M. J. *Amino Acids* **2003**, *25*, 259–274.
(2) Hawkins, C. L.; Davies, M. J. *Chem. Res. Toxicol.* **2002**, *15*, 83–92.
(3) Rees, M. D.; Hawkins, C. L.; Davies, M. J. *J. Am. Chem. Soc.* **2003**, *125*, 13719–13733.
(4) Armesto, X. L.; Canle, M. L.; Garcia, M. V.; Santaballa, J. A. *Chem. Soc. Rev.* **1998**, *27*, 453–460.
(5) Grob fragmentation: Hand, V. C.; Synder, M. P.; Margerum, D. W. *J. Am. Chem. Soc.* **1983**, *105*, 4022–4030.
(6) Elimination reactions: Meng, Q.; Thibblin, A. *J. Am. Chem. Soc.* **1997**, *119*, 1224–1230.
(7) Nucleophilic substitution reactions: Calvo, P.; Crugeiras, J.; Rios, A.; Rios, M. A *J. Org. Chem.* **2007**, *72*, 3171–3178.
(8) Davies, M. J.; Dean, R. T. *Radical-Mediated Protein Oxidation; from chemistry to medicine*; Oxford University Press: Oxford, 1997; 1443.
(9) Deborde, M.; von Gunten, U. *Water Res.* **2008**, *42*, 13–51.

10.1021/jo900349e CCC: $40.75
Published on Web 03/23/2009

SCHEME 1. Intramolecular Rearrangement Reactions in Chloramine-Derived Nitrogen-Centered Radicals

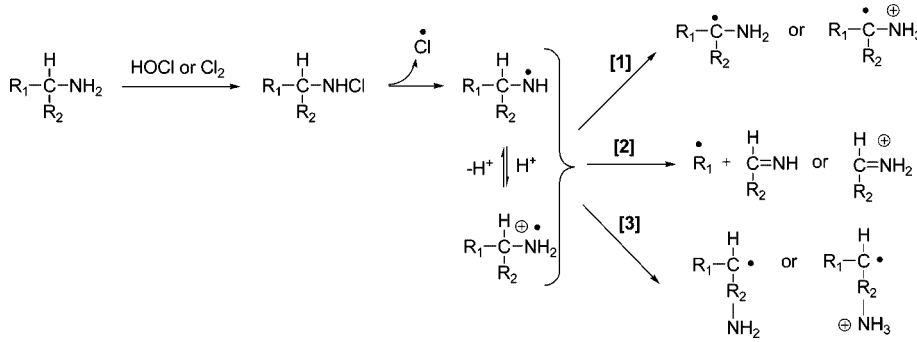

municipal wastewaters in recent years.[11−15] Only in a few cases has direct evidence for the formation of chloramine-derived nitrogen-centered radicals in pharmaceuticals been obtained.[16] Experimental evidence for the occurrence of the rearrangement processes described in Scheme 1 is rather scarce, despite the fact that these reactions may play an important role in the fate of pharmaceutical residues in aqueous environments. As a prelude to a broader computational investigation of radical rearrangements in amine-containing pharmaceuticals, we have now computed thermochemical parameters associated with intramolecular hydrogen shifts in piperidine and its substituted derivatives. Piperidines represent a class of heterocycles frequently associated with biologically active natural products and are often incorporated as the key structural motif in a vast array of pharmaceuticals. Piperidine ring model systems allow intramolecular 1,2-, 1,3-, and 1,4-hydrogen migrations to be examined in detail. For comparison, the corresponding intramolecular hydrogen atom shifts in aliphatic amine radical cations have been examined both experimentally and computationally.[17−19] It has been shown that H-atom transfer steps often precede skeletal rearrangements of amine radical cations, such as nitrogen atom migration or fragmentation by C−C bond cleavage. Interestingly, only acyclic aliphatic amine radicals were investigated, and no comparable studies for cyclic amine radicals were reported. A study of energetically feasible rearrangement pathways in heterocycles such as piperidine, pyrrolidine, or piperazine thus appears timely and appropriate. Interest in assessing the ecological risk of chloramine-pharmaceuticals continues unabated and computational techniques can fruitfully complement these experimental/analytical studies by modeling reaction mechanisms and rearrangement pathways that could be important in understanding the chemical fate of choramine-derived radicals in the environment.

Results and Discussion

The experimental pK_a value of 5.8 (±0.5) suggests that, contrary to the parent molecule,[20] piperidine radical (**1a/1b**) in aqueous solution prefers a neutral structure, while the radical cation becomes the dominant species below pH = 5. However, both piperidine radical and radical cation coexist in slightly acidic media (pH ≈ 6) and therefore should be considered together when exploring feasible rearrangement processes, such as hydrogen migrations (Scheme 2), relevant to their chemical fate in aqueous environment. It is quite generally known that protonation of neutral aminyl radicals strongly affects the reactivity and the selectivity of these species.[21−24,28]

The performance of a variety of methods for calculating the thermochemistry of hydrogen migration was assessed. We use G3B3 and G3(MP2)-RAD as our reference procedures in order to evaluate the efficiency of other high-level methods (Tables 1 and 2). The latter method, which is quite cost-effective and gives essentially the same results as G3B3 (see Tables 1 and 2), has recently been optimized for open-shell systems.[25,26] The accuracy of G3B3 and G3(MP2)-RAD methods has been tested by calculating the pK_a of piperidine and pyrrolidine radical cations for which experimental values are known (pK_a = 5.8 and 5.4, respectively). The combination of G3(MP2)-RAD (or G3B3) energies, with thermochemical corrections calculated at the (U)B3LYP/6-31g(d) level, and the solvation free energies from the CPCM/UAHF procedure (optimization in model solvent, ε = 78.4) yields pK_a values that are in excellent agreement with experimental results (Table 1; see also the Supporting Information). We made use of the thermodynamic cycle shown in Scheme 3 and eqs 1 and 2. According to the

(10) (a) Li, J.; Blatchley, E. R., III. *Environ. Sci. Technol.* **2007**, *41*, 6732–6739. (b) Fiss, E. M.; Rule, K. L.; Vikesland, P. J. *Environ. Sci. Technol.* **2007**, *41*, 2387–2394. (c) Joo, S. H.; Mitch, W. A. *Environ. Sci. Technol.* **2007**, *41*, 1288–1296.
(11) Khetan, S. K.; Collins, T. J. *Chem. Rev.* **2007**, *107*, 2319–2364.
(12) Glassmeyer, S. T.; Shoemaker, J. A. *Bull. Environ. Contam. Toxicol.* **2005**, *74*, 24–31.
(13) Bedner, M.; MacCrehan, W. A. *Chemosphere* **2006**, *65*, 2130–2137.
(14) Dodd, M. C.; Huang, C.-H. *Environ. Sci. Technol.* **2004**, *38*, 5607–5615.
(15) Dodd, M. C.; Shah, A. D.; von Gunten, U.; Huang, C.-H. *Environ. Sci. Technol.* **2005**, *39*, 7065–7076.
(16) Zhang, H.; Huang, C.-H. *Environ. Sci. Technol.* **2005**, *39*, 4474–4483.
(17) Hammerum, S.; Nielsen, C. B. *J. Phys. Chem. A* **2005**, *109*, 12046–12053.
(18) Janovsky, I.; Knolle, W.; Naumov, S.; Williams, F. *Chem. Eur. J.* **2004**, *10*, 5524–5534.
(19) Yates, B. F.; Radom, L. *J. Am. Chem. Soc.* **1987**, *109*, 2910–2915.
(20) The experimental pK_a value of piperidine is 11.1 (±0.3). (a) Perrin, D. D. In *Dissociation Constants of Organic Bases in Aqueous Solutions*; Butterworths: London, 1965. (b) Searles, S.; Tamres, M.; Block, F.; Quarterman, L. A. *J. Am. Chem. Soc.* **1956**, *78*, 4917–4920. (c) Hall, H. K. *J. Am. Chem. Soc.* **1957**, *79*, 5441–5444.
(21) Gauld, J. W.; Radom, L. *J. Am. Chem. Soc.* **1998**, *119*, 9831–9839.
(22) Wagner, B. D.; Ruel, G.; Lusztyk, J. *J. Am. Chem. Soc.* **1996**, *118*, 13–19.
(23) Musa, O. M.; Horner, J. H.; Shahin, H. E.; Newcomb, M. *J. Am. Chem. Soc.* **1996**, *118*, 3862–3868.
(24) Horner, J. H.; Martinez, F. M.; Musa, O. M.; Newcomb, M.; Shahin, H. E. *J. Am. Chem. Soc.* **1995**, *117*, 11124–11133.
(25) Henry, D. J.; Parkinson, C. J.; Radom, L. *J. Phys. Chem. A* **2002**, *106*, 7927–7936.
(26) Curtiss, L. A.; Raghavachari, K.; Redfern, P. C.; Rassolov, V.; Pople, J. A. *J. Chem. Phys.* **1998**, *109*, 7764–7776.
(27) Jonsson, M.; Wayner, D. D. M.; Lusztyk, J. *J. Phys. Chem.* **1996**, *100*, 17539–17543.
(28) Moran, D.; Jacob, R.; Wood, G. P. F.; Coote, M. L; Davies, M. J.; O'Hair, R. A. J.; Easton, C. J.; Radom, L. *Helv. Chim. Acta* **2006**, *89*, 2254–2272.
(29) See, for example: Hammerum, S.; Henriksen, T. *Int. J. Mass Spectrom.* **2000**, *199*, 71–78.

SCHEME 2. Stationary Points for [N↔C]-H Shifts in Piperidine Radicals Located at the Corresponding Energy Surface

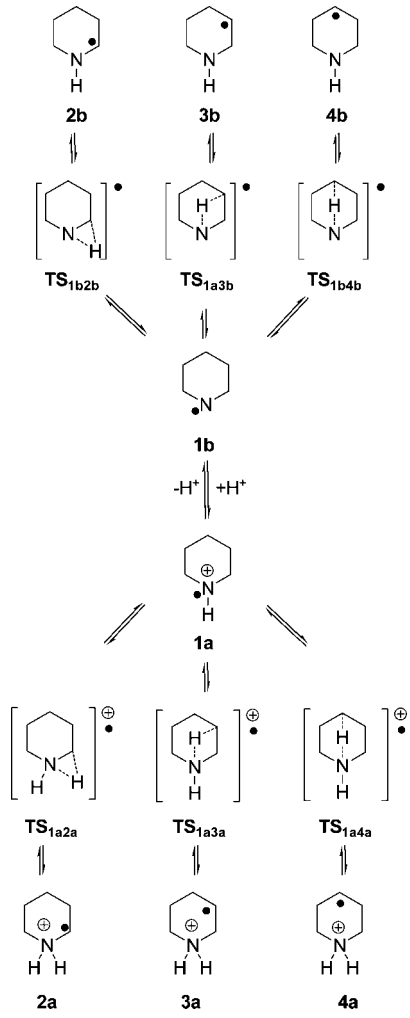

SCHEME 3. Free Energy Cycle for the Calculation of pK_a Values of Pyrrolidine (n = 1) and Piperidine (n = 2) Radical Cations in Aqueous Solution

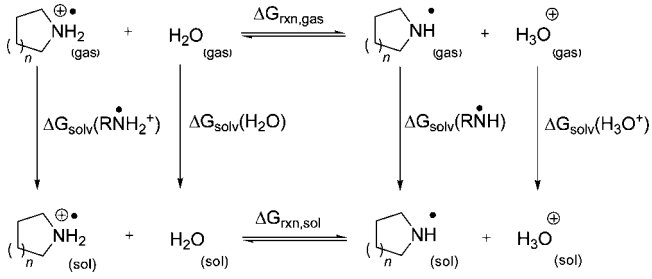

free energy cycle (Scheme 3), the overall expression for the reaction free energy for proton transfer from the radical cation to the solvent is

$$\Delta G_{rxn,sol} = \Delta G_{rxn,gas} + \Delta G_{solv}(RNH^{\bullet}) + \Delta G_{solv}(H_3O^{+}) - \Delta G_{solv}(RNH_2^{+\bullet}) - \Delta G_{solv}(H_2O) \quad (1)$$

and

$$pK_a = \Delta G_{rxn,sol}/2.303RT - \log[H_2O] \quad (2)$$

SCHEME 4. Schematic G3B3 Potential Energy Profile for Hydrogen Migrations in Piperidine Radical Cations in the Gas Phase ([N↔C]-H Shifts, Solid Lines; [C↔C]-H Shifts, Dashed Lines)

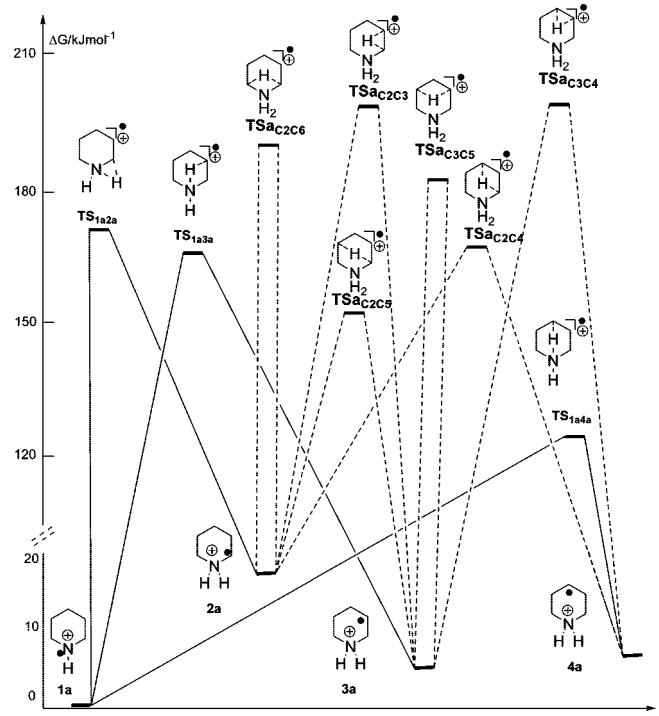

In addition, very accurate results in reproducing the experimental gas-phase basicity (920.4 kJ/mol) for the parent piperidine (closed shell system) were obtained again by using both G3B3 and G3(MP2)-RAD methods (921.8 and 922.0, respectively; see the Supporting Information). The corresponding pK_a value for piperidine was calculated in reasonable agreement with experiment (pK_a = 11.1) by using G3B3 (pK_a = 9.3) and G3(MP2)-RAD methods (pK_a = 9.5). If experimental values of solvation free energies of H_2O and H_3O^+ are included in eq 1, much better agreement is obtained for piperidine, i.e., pK_a = 10.9 using the G3B3 method and pK_a = 11.2 using the G3(MP2)-RAD method (see the Supporting Information).

Piperidine Radical Cation. In the search for the most favorable rearrangement process in piperidine-derived radicals, we have located a number of stationary points which correspond to intramolecular hydrogen migrations. Both [N↔C]− and [C↔C]-hydrogen shifts in piperidine radicals were considered (Schemes 2 and 4). A number of different transition states are located for [C↔C]-H shifts in the piperidine radical cation (Scheme 4), but only the lower energy structures were considered for comparative study.

Similar to earlier studies,[17−19,28] the calculated barriers for [N↔C]-H shifts in piperidine radical cation decrease as the ring size in the corresponding cyclic transition-state structures increases. For example, at the G3B3 level the calculated energy barrier for 1,2-, 1,3-, and 1,4-[N↔C]-H shifts are 175.4, 167.8, and 124.9 kJ/mol, respectively. This sequence is in line with experimental data, which have shown that reactions involving larger transition-state structures are strongly preferred.[18,29−31]

(30) See, for example: Bjørnholm, T.; Hammerum, S.; Kuck, D. *J. Am. Chem. Soc.* **1988**, *110*, 3862–3869.

(31) See, for example: Corey, E. J.; Hertler, W. R. *J. Am. Chem. Soc.* **1960**, *82*, 1657–1668.

TABLE 1. Free Energy of Proton Transfer from Radical Cations (of Eq 1) to Water Calculated at Various Levels of Theory (at 298.15 K and 1 atm): Calculation of pK_a Values Is Based on the Gas-Phase Free Energy Data and Aqueous Solvation Free Energies for Individual Components (of Eq 1) Obtained from the CPCM/UAHF/UB3LYP/6-31G(d) Model

	(U)B3LYP/6-31G(d)	(U)CCSD(T)/6-31G(d)	G3(MP2)-RAD	G3B3	exp
	pyrrolidine radical cation ($n = 1$)				
$\Delta G_{rxn,gas}$	229.8	223.1	234.1	232.8	
$\Delta G_{rxn,sol}$	38.0	31.3	42.3	40.9	
pK_a	4.9	3.7	5.7	5.4	5.5 (±0.5)[27]
	piperidine radical cation **1a** ($n = 2$)				
$\Delta G_{rxn,gas}$	245.8	234.6	246.5	246.1	
$\Delta G_{rxn,sol}$	42.3	31.1	42.9	42.6	
pK_a	5.6	3.7	5.8	5.7	5.8 (±0.5)[27]

TABLE 2. Relative Energies ΔG (in kJ/mol; at 298.15 K) for Stationary Points in the Hydrogen Migration Reactions of Piperidine Radical Cation (1a)

	minimum structures				TS structures for [N↔C] shifts			TS structures for [C↔C] shifts[a]		
method[c]	**1a**	**2a**	**3a**	**4a**	TS_{1a2a}	TS_{1a3a}	TS_{1a4a}	TSa_{C2C3}	TSa_{C2C6}	TSa_{C2C5}
UB3LYP/6-31G(d)	0.0	35.6	19.4	21.6	189.1	179.6[b]	133.9	216.6	210.5	172.9
B3LYP/G3MP2large	0.0	27.2	12.9	14.9	176.6	174.6	129.3	200.6	200.2	162.9
ROMP2/6-31G(d)	0.0	7.7	−7.6	−6.2	170.3	155.5	114.3	194.8	183.9	147.2
ROMP2(FC)/G3MP2large	0.0	2.2	−12.1	−10.8	152.6	142.9	99.4	170.9	163.0	124.5
UCCSD(T)/6-31G(d)	0.0	21.7	6.2	7.6	191.4	180.4	138.4	217.1	206.9	170.8
G3(MP2)RAD	0.0	16.2	1.6	3.0	173.7	168.1	123.5	193.2	186.0	148.1
G3B3	0.0	16.7	2.2	3.6	175.4	167.8	124.9	196.1	190.6	152.4
$-\Delta G_{solv}$[d]	260.8	271.7	278.2	280.6	252.5	236.8	234.1	262.3	259.1	260.6
G3B3 + ΔG_{solv}	0.0	5.8	−15.2	−16.2	183.7	191.8	151.6	194.5	192.3	152.6

[a] Only lower energy structures are included. [b] The structure in chair conformation. [c] All energies have been calculated for UB3LYP/6-31G(d) geometries. [d] Solvation energies calculated with CPCM/UAHF/UB3LYP/6-31G(d) method. Full geometry optimizations with continuum model have been performed for all species in the model solvent of $\varepsilon = 78.4$.

The calculated energy barriers for [C↔C]-H shifts in piperidine radical cations also decrease in the order 1,2- > 1,3- > 1,4-hydrogen shift. However, these [C↔C]-H shifts were calculated to have higher barriers, in average by about 30 kJ/mol, than the corresponding [N↔C]-H shifts. At the G3B3 level, the transition-state structure for 1,4-[C↔C]-H shift is found to be 27.5 kJ/mol higher in energy than the corresponding transition state structure for 1,4-[N↔C]-H shift.

Interestingly, in the case of neutral piperidine radical some of [C↔C]-H shifts are energetically more favored (see below) than [N↔C]-H shifts, suggesting that in neutral radicals different rearrangement mechanisms could be operative. Transition state structures for 1,2-, 1,3-, and 1,4-[N↔C]-H shifts in piperidine radical cation, located at the UB3LYP/6-31G(d) level, are characterized by N−H−C bridging in which the N−H and C−H bonds are elongated (Figure 1). The relatively large imaginary frequencies (all above 1500*i* cm^{-1}; see the Supporting Information) correspond to the movement of the bridging hydrogen atom between nitrogen and carbon. The value of the calculated transfer angle N−H−C decreases with decreasing ring size (Figure 1). Therefore, significant ring strain is expected in the 3- and 4-membered ring transition structures involved in 1,2- and 1,3-shifts, respectively. This indicates that 1,4-[N↔C]-H shifts will dominate hydrogen migrations in piperidine radical cation in the gas phase. To characterize the 1,4-[N↔C]-H shift in more detail, we have monitored the migrating hydrogen atom partial charge and spin density along the reaction pathway (Figure 2). The IRC calculations starting from the transition state structure TS_{1a4a} confirm that no intermediate exists along the reaction pathway **1a** → **4a**, i.e., that the electron and proton transfer occurs as one kinetic step. Analysis of the partial charge (NPA values) and spin density distribution along the 1,4-[N↔C]-H migration pathway as calculated by UB3LYP/6-31G(d) method reveals that the migrating hydrogen carries a positive charge throughout the reaction **1a** → **4a**. Simultaneously, only negligible unpaired spin density is located on the migrating hydrogen, suggesting that spin flows directly from the nitrogen in **1a** to the C4 carbon atom in **4a** in the course of the reaction. The intramolecular hydrogen migration in **1a** could be described as an associative process (S_H2-like) in which the migrating hydrogen is bonded either to carbon or to nitrogen throughout the reaction channel. This is represented by the SOMO in TS_{1a4a} (Figure 3) that mostly includes N and C4 atoms with some delocalization (0.008) over the migrating H.

Similar electronic properties were calculated for transition-state structures of other distant [N↔C]− and [C↔C]-H shifts (Table 3). It is evident that with decreasing ring size of the cyclic transition-state structure the migrating H charge increases, indicating a larger heterolytic component involved in lower order H-shifts.

In general, activation barriers for hydrogen migrations in piperidine radical cations are higher than in structurally related acyclic amine radical cations,[17−19] suggesting that heterocyclic radicals are less reactive species, at least with respect to intramolecular rearrangements. For example, at the UB3LYP/6-31G(d) level (Table 2) the calculated energy barrier for the intramolecular 1,4-H transfer in piperidine radical cation **1a** is 133.9 kJ/mol (127.7 kJ/mol, based on ZPE-corrected total energy), whereas the corresponding barriers in *n*-propyl- and *N*-methylbutyl radical cations are only 71.6 kJ/mol (B3LYP/6-31G(d) level)[18] and 56.0 kJ/mol (UMP2/6-31+G(d,p) level),[17] respectively.

In the case of primary amines, the distonic radical cations are more stable than their conventional isomers.[17−19,32] However, in the case of piperidine the [N↔C]-hydrogen migrations

(32) Wesdemiotis, C.; Danis, P. O.; Feng, R.; Tso, J.; McLafferty, F. W. *J. Am. Chem. Soc.* **1985**, *107*, 8059–8066.

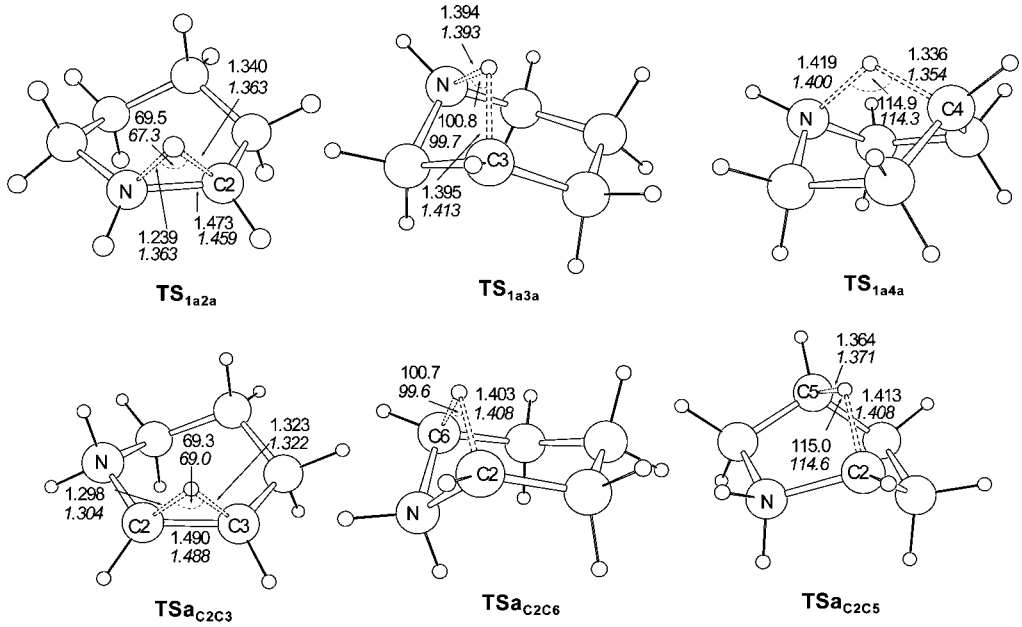

FIGURE 1. UB3LYP/6-31G(d) transition-state structures $\mathbf{TS_{1a2a}}$, $\mathbf{TS_{1a3a}}$, and $\mathbf{TS_{1a4a}}$ for 1,2-, 1,3-, and 1,4-[N↔C]-H shifts, respectively, and transition-state structures $\mathbf{TSa_{C2C3}}$, $\mathbf{TSa_{C2C6}}$, and $\mathbf{TSa_{C2C5}}$ for 1,2-, 1,3-, and 1,4-[C↔C]-H shifts, respectively, in piperidine radical cation (distances are in angstroms, bond angles are in degrees; CPCM/UAHF/UB3LYP/6-31G(d) values are in italics; only the most stable conformers/isomers are presented).

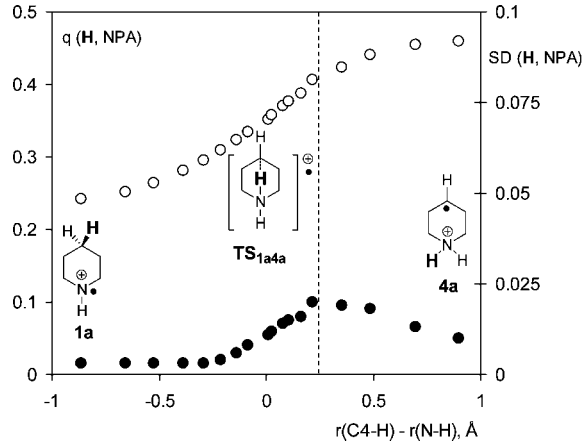

FIGURE 2. Variation of the migrating hydrogen atom (label in bold) charge (NPA value, open cirles) and spin density (filled circles) along the 1,4-[N↔C]-H migration pathway **1a** → $\mathbf{TS_{1a4a}}$ → **4a** as calculated at the UB3LYP/6-31G(d) level.

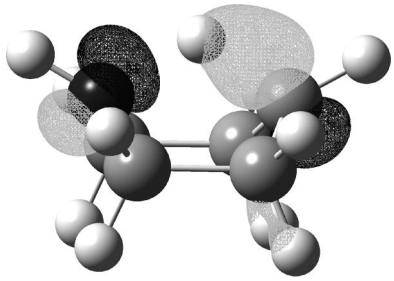

FIGURE 3. Singly occupied molecular orbital in $\mathbf{TS_{1a4a}}$ calculated at the UB3LYP/6-31G(d) level.

favor formation of the N-centered radical, unless solvent effects are included (see below). N-Centered radical **1a** is stabilized by interaction between unpaired spin orbital centered at nitrogen and C2−C3 and C5−C6 bonds. These bonds are calculated

TABLE 3. Migrating Hydrogen Charges and Spin Densities (NPA Values) for Transition-State Structures and Products in [N↔C]− and [C↔C]-H Shift[a] Reactions in Piperidine Radical Cation, As Calculated at the UB3LYP/6-31G(d) Level

structure	*q*(H)/*e*	SD(H)
$\mathbf{TS_{1a2a}}$	0.445	0.013
$\mathbf{TS_{1a3a}}$	0.341	0.012
$\mathbf{TS_{1a4a}}$	0.335	0.008
$\mathbf{TSa_{C2C3}}$	0.381	0.058
$\mathbf{TSa_{C2C6}}$	0.273	0.077
$\mathbf{TSa_{C2C5}}$	0.255	0.070
2a	0.464	0.036
3a	0.465	0.002
4a	0.462	0.002

[a] Only the lower energy transition-state structures for different [C↔C]-H shifts were considered.

SCHEME 5. Spin Density (in Italics) and Charge Distribution (NPA Values) for N- and C-Centered Piperidine Radical Cations, Calculated with UB3LYP/6-31G(d) Method

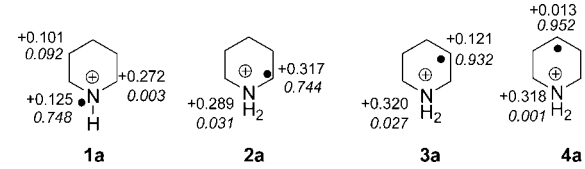

slightly elongated (1.581 Å) at the UB3LYP/6-31G(d) level) as compared to the neutral closed shell piperidine (1.533 Å). In **1a**, the spin is localized on nitrogen with some flow to carbon centers C3 and C5 (Scheme 5), whereas the positive charge is delocalized to adjacent carbon centers C2 and C6. According to the spin density distribution (Scheme 5), only **3a** and **4a** can be classified as distonic radical cations, in which charge and radical sites are spatially separated.[33]

(33) (a) Yates, B. F.; Bouma, W. J.; Radom, L. *J. Am. Chem. Soc.* **1984**, *106*, 5805–5808. (b) Yates, B. F.; Bouma, W. J.; Radom, L. *Tetrahedron* **1986**, *22*, 6225–6234.

Medium Effects. Theoretical studies of implicit solvent effects on rearrangement processes in radical cations are rather scarce. We find here that these effects are to be considered since the relative energies of species involved as well as mechanistic details are significantly changed. If the solvent is implicitly included by using CPCM/UAHF calculations, distonic radicals **3a** and **4a** become more stable than N-centered piperidine radical **1a** (Table 2). Only small changes in the geometries of piperidine radical cations are detected during geometry optimization in the presence of the continuum model solvent (see the Supporting Information). However, the C-centered radicals **2a**−**4a** are better solvated than N-centered radical **1a** (Table 2). The calculated energy difference between transition-state structures for [C↔C]− and [N↔C]-H shifts becomes negligible when the model solvent is applied, suggesting that similar barriers for both types of hydrogen migrations could be expected in polar media. Also, only minor structural changes of transition-state structures on going from the gas phase to the solvent ($\varepsilon = 78.4$) are calculated by CPMC/UAHF optimization (Figure 1).

The results in Table 2 also show that all intermediates involved in rearrangement reactions are solvated better than the respective transition state structures, which results in higher energy barriers both for [C↔C]− and [N↔C]-H shift rearrangements in the continuum model solvent. It thus appears that intramolecular hydrogen migrations in polar solvent become unfavorable processes, unless specific solvent interactions[34−36] mediate the rearrangement process (see below).

To consider specific solvent interactions with intermediates involved in [N↔C]-H shift rearrangements, a discrete water molecule is included in the solvent modeling calculations. A number of studies have reported a mechanism by which distonic radical cations may interconvert with their conventional counterparts through interaction with an appropriate neutral molecule.[37] For the systems under study here, we find that a combination of solvent continuum model (CPCM) and one explicit water molecule significantly reduces the energy barriers for all [N↔C]-hydrogen migrations, whereas the solvent effect on the relative energies between reactants and products is negligible.

Three different water-assisted pathways have been considered: pathway **A** in which the water molecule is bound to the migrating hydrogen throughout the reaction, pathway **B** in which the water molecule is directly involved in forming five-, six-, or seven-membered ring transition states, as required for 1,2-, 1,3-, or 1,4-H transfer, respectively, and pathway **C** in which a "spectator" water molecule is bound to the amine hydrogen throughout the reaction (see an example for 1,2-H transfer in Scheme 6).

Transition-state structures for pathways **A**, **B**, and **C** were located (Figure 4) and were characterized by only one imaginary frequency, which corresponds to hydrogen migration between N- and C-centers. The IRC procedure shows that all transition states lead to the minimum **1w** on the reactant side and water-complexed intermediates (**2w**, **3w**, or **4w)** on the product side. Several different complexes between reactant **1a** and water were

SCHEME 6. Different Pathways for Water-Assisted 1,2-[N↔C]-H Shifts in Piperidine Radical Cation (1w) and Neutral Piperidine Radical (1bw)

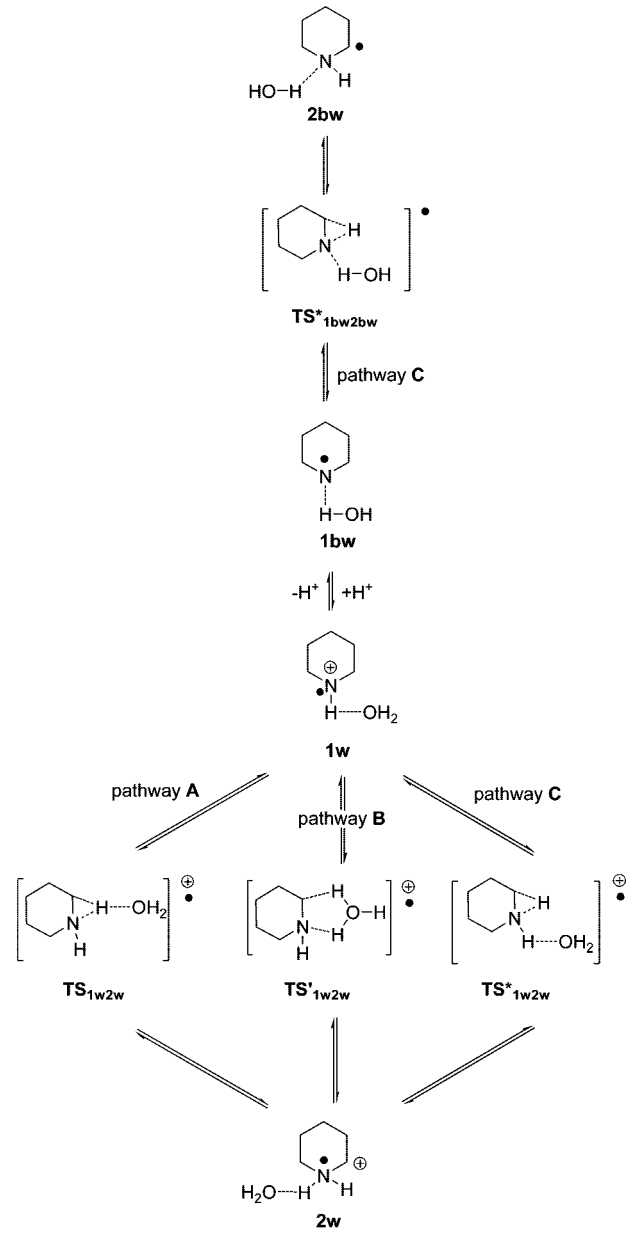

optimized, but all starting geometries converged to water-complexed N-centered radical **1w**. This suggests that all [N↔C]-H shifts in piperidine radical cation start from **1w** in which the NH group is hydrogen-bonded to the explicit water molecule (Schemes 6 and 7).

In general, the calculated energy barriers for all water-assisted pathways (**A**, **B**, and **C**) are lower in energy than the corresponding [N↔C]-H shifts in the gas phase (Tables 2 and 4). Pathway **A**, in which a water molecule is bound to the migrating H atom, is found to be the most feasible process. Interaction with a water molecule (complex of type $H_{migr}\cdots OH_2$) leads to a significant lowering of the barrier for 1,2-, 1,3-, and 1,4-[N↔C]-H shift (Tables 2 and 4). At the G3B3 level (including ΔG_{solv} as estimated by CPCM method), the calculated energy barrier for the water-assisted 1,2-, 1,3-, and 1,4-[N↔C]-H migrations (via pathway **A**) are lowered by 110.4, 80.3, and 31.8 kJ/mol, respectively, as compared to the corresponding

(34) Smith, D. M.; Buckel, W.; Zipse, H. *Angew. Chem., Int. Ed.* **2003**, *42*, 1867–1870.
(35) Gauld, J. W.; Radom, L. *J. Am. Chem. Soc.* **1997**, *119*, 9831–9839.
(36) Mohr, M.; Zipse, H.; Marx, D.; Parrinello, M. *J. Phys. Chem. A* **1997**, *101*, 8942–8948.
(37) (a) Simon, S.; Sodupe, M.; Bertran, J. *Theor. Chem. Acc.* **2004**, *111*, 217–222. (b) Rodriguez-Santiago, L.; Vendrell, O.; Tejero, I.; Sodupe, M.; Bertran, J. *Chem. Phys. Lett.* **2001**, *334*, 112–118. (c) Gauld, J. W.; Audier, H; Fossey, J.; Radom, L. *J. Am. Chem. Soc.* **1996**, *118*, 6299–6300.

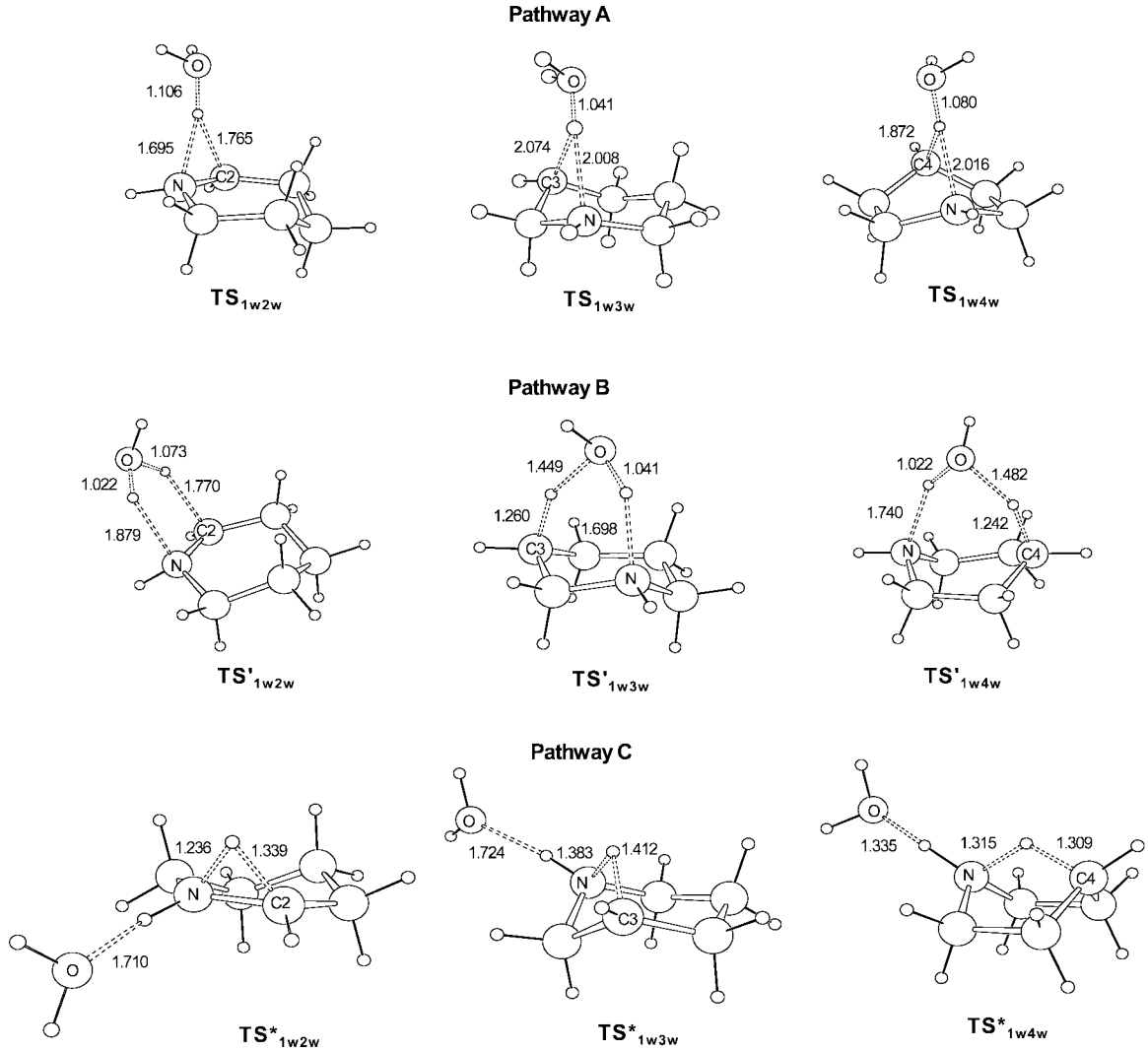

FIGURE 4. UB3LYP/6-31G(d)-optimized geometries of transition-state structures for the water-assisted [N↔C]-H shifts in piperidine radical cations (bond distances are in angstroms). Transition-state structures labeled as **TS**, **TS′**, and **TS*** correspond to pathways **A**, **B**, and **C**, respectively.

TABLE 4. Relative Energies Δ*G* (in kJ/mol; at 298.15 K) for Stationary Points in the Water-Assisted 1,2-, 1,3-, and 1,4-[N↔C]-H Migrations of Piperidine Radical Cation

	structure[a]	UB3LYP	G3B3	$-\Delta G_{solv}$[b]	G3B3 + ΔG_{solv}
	1w	0.0	0.0	219.7	0.0
	TS$_{1w2w}$	181.4	166.6	313.0	73.3 (183.7)[c]
1,2-[N↔C] shift	**TS′$_{1w2w}$**	173.7	170.2	291.7	98.2
	TS*$_{1w2w}$	190.6	178.6	219.3	179.0
	TS$_{1w3w}$	213.0	207.7	315.9	111.5 (191.8)[c]
1,3-[N↔C] shift	**TS′$_{1w3w}$**	175.6	200.8	262.0	158.5
	TS*$_{1w3w}$	185.8	174.2	209.2	184.7
	TS$_{1w3w}$	209.8	208.9	308.8	119.8 (151.6)[c]
1,4-[N↔C] shift	**TS′$_{1w4w}$**	174.5	207.7	276.1	151.3
	TS*$_{1w4w}$	139.5	129.4	205.9	143.2
	2w	38.6	20.8	237.4	3.1 (5.8)[c]
	3w	22.8	5.2	243.5	−18.6 (−15.2)[c]
	4w	26.9	8.4	245.1	−17.0 (−16.2)[c]

[a] Transition-state structures labeled as **TS**, **TS′**, and **TS*** correspond to water-assisted pathways **A**, **B**, and **C**, respectively. [b] Solvation energy calculated with CPCM/UAHF/UB3LYP/6-31G(d) method. Full geometry optimizations with continuum model have been performed for all species in the model solvent of $\varepsilon = 78.4$. [c] Relative energies for the corresponding uncatalyzed hydrogen migrations in aqueous solution are included in parentheses.

uncatalyzed hydrogen migrations. Interestingly, the barrier for hydrogen shift (via pathway **A**) decreases in the order 1,4- > 1,3- > 1,2- (Table 4), in contrast to the uncatalyzed hydrogen migrations in the gas phase (Table 2). Therefore, the 1,4-[N↔C]-H shift is expected to be the most favorable process in the gas phase, whereas the 1,2-[N↔C]-H shift becomes more favored in an aqueous environment (Scheme 7).

Whereas the calculated energy barriers for all [N↔C]-H hydrogen migrations in piperidine radicals are significantly reduced by an appropriate inclusion of one explicit water molecule, the calculated energy differences between N-centered radical reactant and C-centered radical products are very similar in both water-assisted and uncatalyzed reactions (Tables 2 and 4). In the case of the uncatalyzed reaction, the distonic radical cations **3a** and **4a** are calculated as 15.2 and 16.2 kJ/mol, respectively, more stable than the N-centered radical **1a** (Table 2), while in the case of the water-assisted reaction the (now water-complexed) radicals **3w** and **4w** are calculated to be 18.6 and 17.0 kJ/mol more stable than **1w** (Table 4 and Scheme 5). Also, the calculated free energy (G3B3 + ΔG_{solv}) for the reaction **1a** → **2a** is +5.8 kJ/mol, while that for reaction **1w** → **2w** is +3.1 kJ/mol. Therefore, one can conclude that the explicit water molecule influences significantly the kinetics of all [N↔C]-H shifts in piperidine radical **1a**, but not the thermodynamics of

SCHEME 7. Schematic Potential Energy Profile (G3B3 + ΔG_{solv}) for 1,2-, 1,3-, and 1,4-[N↔C]-H Migrations in Piperidine Radical Cation (Water-Assisted Pathway A, Solid Lines; Uncatalyzed Migrations, Dashed Lines) in Water

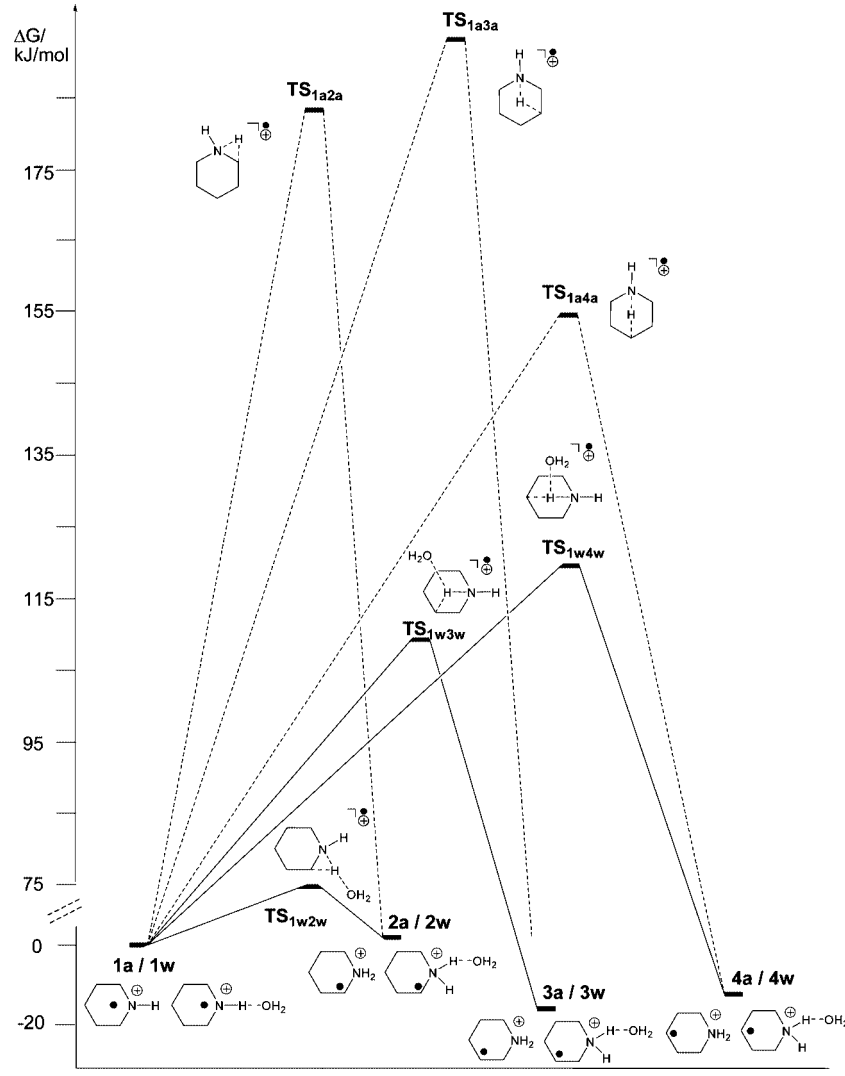

TABLE 5. Relative Energies ΔG (in kJ/mol; at 298.15 K) for Stationary Points in the Hydrogen Migration Reactions of Piperidine Radical 1b

	minimum structures				TS structures for [N↔C] shifts			TS structures for [C↔C] shifts[a]		
method[b]	**1b**	**2b**	**3b**	**4b**	TS_{1b2b}	TS_{1b3b}	TS_{1b4b}	TSb_{C2C3}	TSb_{C2C6}	TSb_{C2C5}
UB3LYP/6-31G(d)	0.0	2.2 (19.3)[c]	36.6	28.9 (31.2)[d]	179.3	184.1 (187.1)[c]	170.2	204.1	214.5	167.9
G3B3	0.0	−13.0 (4.6)	20.9	15.1 (15.8)	166.7	173.0 (176.3)	160.3	186.9	198.1	151.2
$-\Delta G_{solv}$[e]	20.7	23.5	30.9	27.8	21.8	17.5	19.0	24.3	22.9	21.6
G3B3 + ΔG_{solv}	0.0	−10.2	10.7	8.0	165.6	176.2	162.0	183.3	195.9	150.3

[a] Only the lower energy structures were considered. [b] All energies have been calculated for UB3LYP/6-31G(d) geometries. [c] The structure in boat conformation. [d] (N−)H in axial position. [e] Solvation energy calculated with CPCM/UAHF/UB3LYP/6-31G(d) method. Full geometry optimizations with continuum model have been performed for all species in the model solvent of $\varepsilon = 78.4$.

these reactions. In conclusion, the large barriers separating radical cations **1a**−**4a** in the gas phase can be reduced through interaction with one explicit water molecule,[38] which efficiently catalyzes interconversion of these isomeric ions.

Piperidine Radical. In contrast to electrophilic radical cations, which were shown to readily undergo intramolecular hydrogen atom abstraction reactions, the respective neutral radicals are known to be much less reactive. Therefore, it is expected that neutral piperidine radicals **1b**−**4b** are less reactive than protonated piperidine radical cation **1a**.

In several experimental studies, only piperidin-1-yl radical **1b** and piperidin-2-yl radical **2b** have been observed by EPR spectroscopy.[39,40] These experimental findings are supported by our calculations (Table 5), which show that radicals **1b** and **2b** are significantly lower in energy than C-centered piperidin-3-yl (**3b**) or piperidin-4-yl radicals (**4b**). The piperidine radical **2b** is the most stable structure and, as expected,[41,42] is stabilized by interaction of the unpaired electron at the formal C2-radical

(38) The type of catalysis seen in pathway **A** can, in principle, also be expected from other weak Lewis bases such as alcohols and ethers.

(39) Helcke, G. A.; Fantechi, R. *J. Chem. Soc., Faraday Trans. 2* **1974**, *70*, 1912–1919.

(40) Antzutkin, O. N.; Lindgren, M.; Lund, A.; Sjøqvist, L. *J. Chem. Soc., Chem. Commun.* **1992**, 1547.

(41) See, for example: Zipse, H. *Top. Curr. Chem.* **2006**, *263*, 163–189.

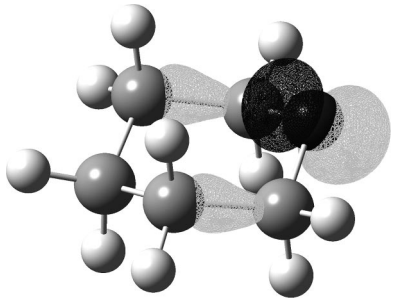

FIGURE 5. UB3LYP/6-31G(d) calculated SOMO of *A′* symmetry in piperidine radical **1b**.

center with energetically and spatially adjacent lone pair electrons at the nitrogen center. This two-center three-electron radical stabilizing interaction is reflected in a shortening (1.403 Å at the B3LYP/6-31G(d) level) of the bond connecting the C2 radical and nitrogen center (as compared to the corresponding bond in the closed-shell parent system piperidine with 1.468 Å). Due to this interaction, the spin density (NPA values) is delocalized over the C2 center (0.787 au) and the adjacent nitrogen atom (0.179 au). In contrast, the unpaired electron is mainly localized on the C3 (0.953 au) and C4 (0.951 au) centers (Scheme 4) in **3b** and **4b**. In the case of the N-centered piperidine radical **1b**, the unpaired electron is in an A′ orbital (Figure 5, ^{2}A′ electronic state with C_s symmetry).[43]

In previous studies,[44] the piperidine radical **2b** has been investigated at the HF and MP2//HF levels, and it has been shown that two different conformers exist on the corresponding potential energy surface, i.e., the piperidine radical having the N−H bond in either axial or equatorial orientation. However, optimization at either the UB3LYP/6-31G(d) or the UMP2(Full)/6-31G(d) level cannot locate the axial structure as a real minimum, which converges back to the more stable equatorial conformer on attempted geometry optimization.

It has also been claimed that the most stable form of piperidine radical **2b** adopts a boat conformation.[39] This conclusion was based on CNDO/2 calculations and Dreiding models. The UB3LYP and G3B3 calculations performed here show that the boat conformer is more than 17 kJ/mol less stable than the corresponding chair conformer in the gas phase (Table 5). In contrast to **2b**, two different conformations can be located for **4b** with axial and equatorial orientations of the N−H bond, respectively. The calculated energy difference between these two conformers is only about 1 kJ/mol. The axial conformer is the minimum, which is directly connected to the transition state for 1,4-[N↔C]-hydrogen shift, as calculated by the IRC procedure. Transition state structures for 1,2-, 1,3-, and 1,4-H shifts in piperidine radical **1b** were located at the UB3LYP/6-31G(d) level and were compared to corresponding transition state structures for hydrogen migrations in its protonated counterpart. Comparable to the case of piperidine radical cations, 1,4-shifts dominate hydrogen migrations in the neutral radical. Transition state structures **TS$_{1b4b}$** and **TSb$_{C2C5}$** for 1,4-[N↔C]- and 1,4-[C↔C]-hydrogen shifts (Figure 6), respectively, have similar geometric parameters as those calculated for **TS$_{1a4a}$** and **TSa$_{C2C5}$** (Figure 1). The N−H−C4 and C2−H−C5 bridgings are characterized by elongated N−H and C−H bonds (between 1.3 and 1.45 Å) and the transfer angle is smaller than 120°. Also, the electronic character of the migration process **1b** → **TS$_{1b4b}$** → **4b** is similar (Figure 7) to the corresponding process in piperidine radical cation **1a** (Figure 2). According to calculated charge and spin density values of the migrating hydrogen along the pathway, one can conclude that hydrogen migration in both cases is an associative process (S_H2-like) in which the migrating hydrogen is bonded either to carbon or to nitrogen throughout the reaction channel.

In the gas phase, the G3B3-calculated energy barriers (Table 5) for all hydrogen shifts in neutral piperidine radicals are significantly higher than the calculated barrier for the 1,4-[N↔C]-H shift (124.9 kJ/mol) in piperidine radical cation **1a**. This suggests that piperidine radical **1a** is kinetically more stable than its protonated form, at least in terms of intramolecular rearrangements. It also indicates that protonation of piperidine radical can promote intramolecular rearrangements by lowering the energy barriers for hydrogen migration reactions. However, in piperidine radical [C↔C]-H migrations become relatively more feasible, suggesting that protonation influences the relative energies of species involved and that the overall mechanism could be perturbed.

Contrary to piperidine radical cation **1a**, no implicit solvent effects are observed in the case of piperidine radical **1b**. Both relative energies of intermediates and transitions-state structures are similar in the gas phase and in water as calculated by the CPCM model (Table 5). The possibility of explicit solvent effects, even though less likely than in reactions of radical cation **1w**, has been tested for the 1,2-[N↔C]-H migration in piperidine radical **1bw**. Interestingly, out of the three different water-assisted pathways **A**, **B**, and **C** identified in reactions of the radical cation systems, only pathway **C** appears to be operative for piperidine radical **1bw**. In this rearrangement, the water molecule acts as a proton donor to the nitrogen throughout the reaction ("spectator" mechanism). The transition-state structure **TS$_{1bw2bw}$**, connecting water-complexed reactant **1bw** and product **2bw** (Scheme 6), has been located and characterized by one imaginary frequency (2032*i* cm^{-1}). It is calculated (G3B3 + ΔG_{solv}) 171.7 kJ/mol less stable than **1bw**. The corresponding energy barrier calculated for 1,2-[N↔C]-H shift in piperidine radical **1b** is 165.6 kJ/mol (Table 5). Therefore, one explicit water molecule showed no catalytic effect on hydrogen migration in the neutral piperidine radical **1bw**, which is quite opposite to the water catalysis observed in the case of its protonated counterpart **1w**.

Conclusions

The performance of a number of computational models for calculating the [N↔C]- and [C↔C]-H migration thermochemistry was assessed. Both G3MP2 and G3B3 models give results which are in overall good agreement with relevant experimental data (such as pK_a values of piperidine and pyrrolidine radical cations as well as pK_a value and gas-phase basicity of piperidine). It is found that both protonation and (explicit) solvent effects can significantly influence the energetics and mechanism of hydrogen migrations in the piperidine ring. The calculated energy barriers for hydrogen migrations in the neutral piperidine radical **1b** are generally higher than the corresponding barriers in piperidine radical cation **1a**. This suggests that the latter is kinetically less stable and readily undergoes intramolecular hydrogen migrations. The calculated energy barriers for hydro-

(42) See, for example: Henry, D. J.; Parkinson, C. J.; Mayer, P. M.; Radom, L. *J. Phys. Chem. A.* **2001**, *105*, 6750–6756.

(43) The ^{2}A″ electronic state is calculated to be over 400 kJ/mol less stable than the ^{2}A′ state (see the Supporting Information).

(44) Wayner, D. D. M.; Clark, K. B.; Rauk, A.; Yu, D.; Armstrong, D. A. *J. Am. Chem. Soc.* **1997**, *119*, 8925–8932.

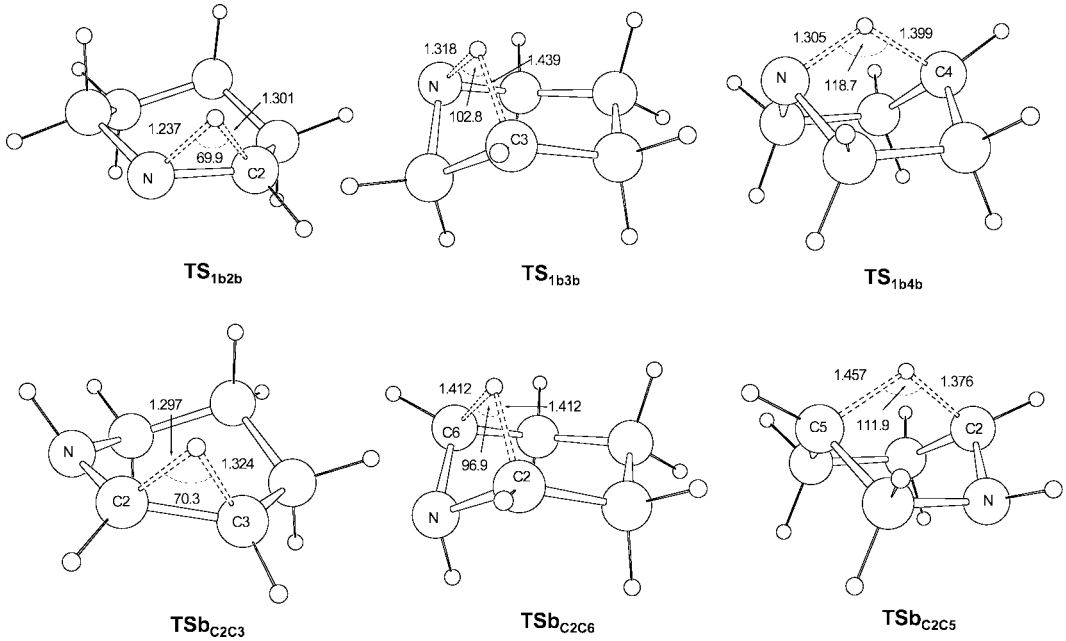

FIGURE 6. UB3LYP/6-31G(d) transition-state structures $\mathbf{TS_{1b2b}}$, $\mathbf{TS_{1b3b}}$, and $\mathbf{TS_{1b4b}}$ for 1,2-, 1,3-, and 1,4-[N↔C]-H shifts, respectively, and transition-state structures $\mathbf{TSb_{C2C3}}$, $\mathbf{TSb_{C2C6}}$, and $\mathbf{TSb_{C2C5}}$ for 1,2-, 1,3-, and 1,4-[C↔C]-H shifts, respectively, in neutral piperidine radical (distances are in angstroms; bond angles are in degrees; only the most stable conformers/isomers are presented).

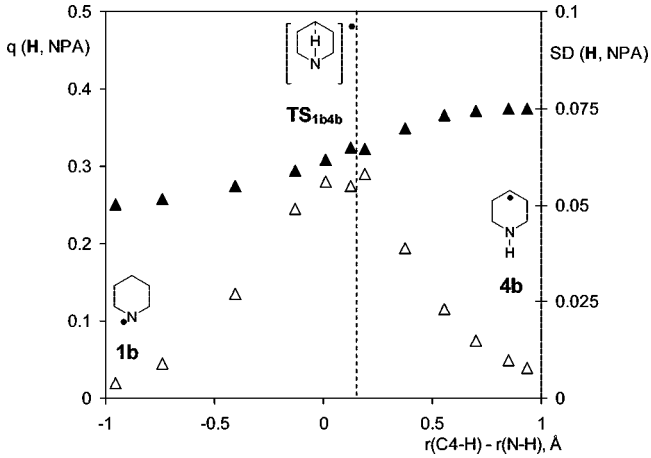

FIGURE 7. Variation of the migrating hydrogen atom charge (NPA value, filled triangles) and spin density (open triangles) along the 1,4-[N↔C]-H migration pathway **1b** → $\mathbf{TS_{1b4b}}$ → **4b** as calculated at the UB3LYP/6-31G(d) level.

SCHEME 8. UB3LYP/6-31G(d) Spin Distributions for Piperidine Radical Isomers

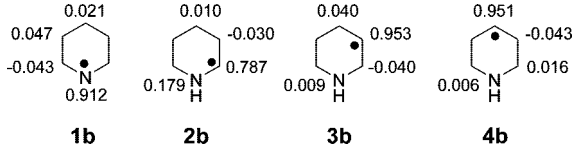

gen shifts in piperidine radical cations are increased when the continuum model solvent (water) is included. On the contrary, when specific solvent interactions are considered the corresponding energy barriers are significantly reduced. Such large medium effects on the reactivity of protonated piperidine radical cations were not observed, neither implicit nor explicit, in the case of neutral piperidine radicals. The calculated energy barriers suggest that [C↔C]-H migrations in piperidine radical **1b** are more favorable than the corresponding [N↔C]-H migrations. Therefore, different rearrangement pathways are to be expected in the piperidine ring system. A careful analysis of solvent effects (both implicit and explicit) and ionization state of the system is mandatory for a detailed description of the overall mechanism.

Computational Details

Geometries of all open-shell systems have been optimized at the UB3LYP/6-31G(d)[45] level of theory. Thermochemical corrections to enthalpies at 298.15 K have been calculated at the same level of theory using the rigid rotor/harmonic oscillator model. Improved energetics have then been calculated with the G3(MP2)-RAD model developed by Radom et al.[46] as well as the G3B3 model by Curtiss et al.[47] Solvation free energies have been determined through geometry optimizations at CPCM/UAHF/UB3LYP/6-31G(d) level.[48,49] Two different basis sets have been employed throughout the text, i.e., the standard 6-31G(d) and the G3MP2large basis set. The latter is the same as 6-311++G(2df,2p) for first-row atoms.[50] The (U)CCSD(T)/6-31G(d) calculations for the G3(MP2)-RAD model have been performed with MOLPRO 2006.1,[51] while

(45) Becke, A. D. *J. Chem. Phys.* **1993**, *98*, 5648–5652.
(46) (a) Henry, D. J.; Parkinson, C. J.; Radom, L. *J. Phys. Chem. A* **2002**, *106*, 7927–7936. (b) Henry, D. J.; Sullivan, M. B.; Radom, L. *J. Chem. Phys.* **2003**, *118*, 4849–4860.
(47) Baboul, A. G.; Curtiss, L. A.; Redfern, P. C.; Raghavachari, K. *J. Chem. Phys.* **1999**, *110*, 7650–7657.
(48) Cossi, M.; Scalmani, G.; Rega, N.; Barone, V. *J. Chem. Phys.* **2002**, *117*, 43–54.
(49) (a) Barone, V.; Cossi, M.; Tomasi, J. *J. Chem. Phys.* **1997**, *107*, 3210–3221. (b) Barone, V.; Cossi, M. *J. Phys. Chem. A* **1998**, *102*, 1995–2001. (c) Amovilli, C.; Barone, V.; Cammi, R.; Cances, E.; Cossi, M.; Mennucci, B.; Pomelli, S.; Tomasi, J. *Adv. Quantum Chem.* **1998**, *32*, 227–262.
(50) Curtiss, L. A.; Redfern, P. C.; Raghvachari, K.; Rassolov, V.; Pople, J. A. *J. Chem. Phys.* **1999**, *110*, 4703–4709.
(51) MOLPRO, version 2006.1, a package of ab initio programs: Werner, H.-J. Knowles, P. J.; Lindh, R.; Manby, F. R.; Schültz, M.; Celani, P.; Korona, T.; Mitrushenkov, A.; Rauhut, G.; Adler, T. B.; Amos, R. D.; Bernhardsson, A.; Berning, A.; Cooper, D. L.; Deegan, M. J. O.; Dobbyn, A. J.; Eckert, F.; Goll, E.; Hampel, C.; Hetzer, G.; Hrenar, T.; Knizia, G.; Köppl, C.; Liu, Y.; Lloyd, A. W.; Mata, R. A.; May, A. J.; McNicholas, S. J.; Meyer, W.; Mura, M. E.; Nicklass, A.; Palmieri, P.; Pflüger, K.; Pitzer, R.; Reiher, M.; Schumann, U.; Stoll, H.; Stone, A. J.; Tarroni, T.; Thorsteinsson, T.; Wang, M.; Wolf, A. See http://www.molpro.net.

all other quantum mechanical calculations have been performed with Gaussian 03, revision D.01.[52]

(52) Frisch, M. J.; Trucks, G. W.; Schlegel, H. B.; Scuseria, G. E.; Robb, M. A.; Cheeseman, J. R.; Montgomery, J. A., Jr.; Vreven, T.; Kudin, K. N.; Burant, J. C.; Millam, J. M.; Iyengar, S. S.; Tomasi, J.; Barone, V.; Mennucci, B.; Cossi, M.; Scalmani, G.; Rega, N.; Petersson, G. A.; Nakatsuji, H.; Hada, M.; Ehara, M.; Toyota, K.; Fukuda, R.; Hasegawa, J.; Ishida, M.; Nakajima, T.; Honda, Y.; Kitao, H.; Klene, M.; Li, X.; Knox, J. E.; Hratchian, H. P.; Cross, J. B.; Bakken, V.; Adamo, C.; Jaramillo, J.; Gomperts, R.; Stratmann, R. E.; Yazyev, O.; Austin, A. J.; Cammi, R.; Pomelli, C.; Ochterski, J. W.; Ayala, P. Y.; Morokuma, K.; Voth, G. A.; Salvador, P.; Dannenberg, J. J.; Zakrzewski, V. G.; Dapprich, S.; Daniels, A. D.; Strain, M. C.; Farkas, O.; Mallick, D. K.; Rabuck, A. D.; Raghavachari, K.; Foresman, J. B.; Ortiz, J. V.; Cui, Q.; Baboul, A. G.; Clifford, S.; Cioslowski, J.; Stefanov, B. B.; Liu, G.; Liashenko, A. Piskorz, P. Komaromi, I. Martin, R. L.; Fox, D. J.; Keith, T.; Al-Laham, M. A.; Peng, C. Y.; Nanayakkara, A.; Challacombe, M.; Gill, P. M. W.; Johnson, B.; Chen, W.; Wong, M. W.; Gonzalez, C.; Pople, J. A. *Gaussian 03, revision D.01*; Gaussian, Inc.: Wallingford, CT, 2004.

Acknowledgment. Financial support for this project by the DFG is gratefully acknowledged. V.V. thanks the AvH Foundation for generous support and the Computing Centre SRCE of the University of Zagreb for allocating computer time on the Isabella cluster where a part of the calculations were performed.

Supporting Information Available: UB3LYP/6-31G(d)- and CPMC/UAHF/UB3LYP/6-31G(d)-optimized geometries, imaginary frequency data, and additional calculated thermochemical data. This material is available free of charge via the Internet at http://pubs.acs.org.

JO900349E